Article:
Edwards, JH orcid.org/0000-0003-4152-6140, Ingham, E orcid.org/0000-0002-9757-3045 and Herbert, A orcid.org/0000-0002-6527-2205 (2019) Decellularisation affects the strain rate dependent and dynamic mechanical properties of a xenogeneic tendon intended for anterior cruciate ligament replacement. Journal of the Mechanical Behavior of Biomedical Materials, 91. pp. 18-23. ISSN 1751-6161

https://doi.org/10.1016/j.jmbbm.2018.11.023

Journal of the Mechanical Behavior of Biomedical Materials 91 (2019) 18–23

Contents lists available at ScienceDirect

Journal of the Mechanical Behavior of Biomedical Materials

journal homepage: www.elsevier.com/locate/jmbbm

Decellularisation affects the strain rate dependent and dynamic mechanical properties of a xenogeneic tendon intended for anterior cruciate ligament replacement

Jennifer Helen Edwards[a,*], Eileen Ingham[a], Anthony Herbert[b]

[a] Institute of Medical and Biological Engineering (iMBE), Faculty of Biomedical Sciences, University of Leeds, Leeds, UK
[b] iMBE, School of Mechanical Engineering University of Leeds, Leeds, UK

ARTICLE INFO

Keywords:
ACL repair
Decellularisation
Strain-rate dependence
Dynamic mechanical analysis

ABSTRACT

Development of new replacement grafts for anterior cruciate ligament (ACL) repair requires mechanical testing to ensure they can provide joint stability following implantation. A decellularised porcine superflexor tendon (pSFT) has been developed previously as an alternative to current reconstruction methods and subjected to biomechanical analysis. The application of varied strain rates to biological tissues is known to alter their biomechanical properties, however the effects of decellularisation on strain rate dependent and dynamic mechanical behaviour of tissues have not been explored. This study utilised tensile testing to investigate the material properties of native and decellularised pSFTs at three different strain rates (1%.s^{-1}, 10%.s^{-1} and 100%.s^{-1}). In addition, dynamic mechanical analysis (DMA) was used to ascertain the relative contributions of the solid and fluid phase components of the tissues.

Ultimate tensile strength was significantly reduced in decellularised compared with native untreated pSFTs but was unaffected by strain rate. In contrast, toe region moduli increased with increasing strain rate for native tissues, but this effect was not observed in decellularised pSFTs. Linear region moduli were unaffected by strain rate, but were significantly reduced in decellularised pSFT compared with native tissue.

Following DMA, significant reductions in dynamic modulus, storage modulus and loss modulus were seen in decellularised compared with native pSFT. Interestingly, the damping ability of the tendons was unaffected by decellularisation, suggesting that solid and fluid phases of the tissue were affected equally. These results, alongside previous studies, suggest that decellularisation affects collagen crimp, tissue swelling and collagen fibre sliding. However, despite these findings, the biomechanical properties of decellularised pSFT remain sufficient to act as an off-the-shelf solution for ACL reconstruction.

1. Introduction

The anterior cruciate ligament (ACL) is of great importance for stabilisation of the knee, preventing anterior displacement of the femur in relation to the tibia (Kiapour and Murray, 2014). When ruptured, there is a need to surgically replace the ligament, to restore function and stability within the knee joint. Gold standard treatments include the use of autograft or allograft tissues (Macaulay et al., 2012), which may be tendon only (such as hamstring tendon) or incorporate bone attachment sites (as with bone-patellar tendon-bone grafts). Both treatment options have potential limitations which must be considered in combination with the circumstances of the patient. Autograft tissues necessitate additional surgery and can lead to donor site morbidity (Joyce et al., 2015), while dead donor cells present in allograft tissues may cause inflammation, leading to a delay in healing (Pinkowski et al., 1996).

One of the promising alternatives to traditional autograft and allograft techniques is the use of off-the-shelf decellularised biological scaffolds. Removing the cellular component of graft tissues reduces the risk of graft rejection and has the potential to accelerate biological incorporation. The extracellular matrix (ECM) component remains to provide mechanical strength and functionality, whilst also acting as a scaffold structure for endogenous cells to populate. Decellularisation processes typically include washes with a series of buffers, including a detergent step and some have been shown to alter the biomechanical properties of tissues (Crapo et al., 2011; Gilbert et al., 2006). One method, developed within this group, involves low concentration detergent washes (0.1% w/v sodium dodecyl sulphate) to disrupt cell

* Corresponding author.
E-mail address: j.h.edwards@leeds.ac.uk (J.H. Edwards).

https://doi.org/10.1016/j.jmbbm.2018.11.023
Received 22 June 2018; Received in revised form 2 November 2018; Accepted 23 November 2018
Available online 26 November 2018
1751-6161/

membranes, nuclease treatments to break down released DNA and protease inhibitors to prevent breakdown of the tissue ECM. This has been successfully applied to a variety of tissues, including heart valves (Booth et al., 2002; Knight et al., 2005), meniscus (Stapleton et al., 2008) and tendons (Herbert et al., 2015; Jones et al., 2017).

These studies have suggested that decellularisation creates a more open and porous ECM, accompanied by a decrease in interstitial fluid viscosity within the tissue and an increase in fluid flow (Herbert et al., 2015). It is paramount that appropriate biomechanical performance is provided by a decellularised ACL graft tissue to function under physiological conditions. These conditions vary considerably depending on the activity and lifestyle of the individual patient. Given the observed changes in interstitial fluid viscosity, it is important to determine if this adversely affects decellularised ACL graft tissue performance under varying strain rates and dynamic loading.

The intricate structural architecture of biological tissues (comprising of cells and ECM matrix proteins such as collagen and proteoglycans) gives rise to their viscoelastic properties (Clemmer et al., 2010) and it has been well documented that the strain rate applied to a biological tissue can affect the material properties observed during mechanical testing. Human brain tissue has previously been shown to have increased tensile, compressive and shear moduli with increasing strain rate (Jin et al., 2013). Strain rate dependent effects have also been shown for abdominal wall tissue (Ben Abdelounis et al., 2013), spinal ligaments (Mattucci et al., 2012, 2013), skin (Ottenio et al., 2015), and spinal cord (Fradet et al., 2016). In addition, Dynamic Mechanical Analysis (DMA) may also be used as an investigative technique to determine the rate-dependent properties of biological tissues using different applied frequencies. An oscillating stress is applied to the sample and the corresponding oscillatory strain response is recorded. This data allows calculation of the material's elastic (in phase) and viscous (out of phase) responses. For example, DMA has previously been used to examine the viscoelastic behaviour of corneal (Hatami-Marbini and Rahimi, 2015), brain (MacManus et al., 2015) and tendon (Nagasawa et al., 2008) tissues.

To date, the effects of strain rate on biological tissues following decellularisation remains relatively unexplored. This study aimed to address this shortfall by determining the material properties of previously reported decellularised porcine superflexor tendons (pSFTs) (Jones et al., 2017) at three different strain rates and compare any rate dependent response to untreated control pSFTs. In the previous study, the pSFT was selected due to the ease of harvest from tissue obtained routinely from the abattoir, in dimensions suitable for ACL repair. Furthermore, by determining the dynamic mechanical properties (dynamic modulus, storage modulus, loss modulus) of decellularised and untreated pSFT tissues, this study investigated the contributions of solid and fluid phases to their biomechanical properties.

2. Materials and methods

2.1. Tissue sourcing and decellularisation

Forty-eight female ~70 kg, 4 month old, large white pigs were obtained from a local abattoir (J Penny, Leeds, UK) within 24 h of slaughter. pSFT's were removed and stored at −20 °C with phosphate buffered saline (PBS) soaked filter paper prior to decellularisation and/or testing. 24 specimens were decellularised by using a previously established procedure (Jones et al., 2017; Herbert et al., 2015), including antibiotic treatment, acetone washes, low concentration detergent (sodium dodecyl sulphate (SDS), 0.1% w/v) washes and nuclease treatments. The process also included PBS washes and a 0.1% peracetic acid sterilisation step in the final stages. The remaining 24 specimens were left in storage at −20 °C as untreated native controls.

2.2. Biomechanical testing

2.2.1. Specimen preparation

For each group investigated ($n = 6$), pSFT's were removed from storage and immersed in dry ice to aid processing them into dumbbell shapes with a working cross-sectional area of ~3.5 × 5 mm and gauge length of 30 mm. All specimens were then wrapped in PBS soaked filter paper and allowed to thaw and equilibrate at room temperature for at least two hours prior to mechanical testing. Once fully thawed and hydrated, the width, depth and length of each tendon was determined by calculating the average of three measurements using digital Vernier callipers. This method of measurement has previously been shown to produce results comparable to laser micrometer systems in similar tissues (Woo et al., 1990).

2.2.2. Study 1: Failure testing under varying strain rates

Strain rate dependent biomechanical properties before and after decellularisation were investigated by tensile testing of pSFT grafts to failure. A total of 18 native and 18 decellularised pSFT were split into smaller groups (n = 6) and assigned to one of three different strain rates; $1\%.s^{-1}$, $10\%.s^{-1}$ and $100\%.s^{-1}$. Specimens were mounted via bespoke 'cyro-grips' to an Instron ElectroPuls E10, 000 (Instron, Bucks, UK) materials testing machine equipped with a 10 kN load cell (Fig. 1a). This method has been used successfully in previous studies for gripping pSFT's during tensile testing (Edwards et al., 2016; Herbert et al., 2015). As a precautionary measure, a probe measured the temperature of the specimens at their gauge length immediately prior to testing, to ensure they had remained at room temperature.

Once secured in the testing apparatus, specimens were pre-conditioned for 10 cycles at a frequency of 0.5 Hz between 0 and 50 N under load control. Following these preconditioning cycles, specimens underwent a ramp to failure at a pre-selected strain rate. Data was recorded at a frequency of 10 Hz. Engineering stress (σ) was calculated by dividing the force recorded by the load cell by the original cross-sectional area (width x thickness) at the specimen gauge length, whereas engineering strain (ε) was determined by dividing the crosshead displacement by the original specimen gauge length.

Stress-strain data was then fitted to a bi-linear model using non-linear least squares regression with a custom written Matlab script (Herbert et al., 2016) (Fig. 1b). Similar bi-linear constitutive models have previously been used for biological tissues including tendon (Chandrashekar et al., 2008; Lynch et al., 2003), diaphragm (Gaur et al., 2016) and spinal ligaments (Mattucci et al., 2012). In addition to elastic moduli representing the toe region and linear region, the transition point (ε_T, σ_T) between the toe region and the linear region was determined, where ε_T is the transition strain and σ_T is the transition stress. Finally, the ultimate tensile strength (*UTS*) and strain at failure were also determined.

2.2.3. Study 2: Dynamic Mechanical Analysis

For dynamic mechanical analysis (DMA), native and decellularised specimens (n = 6 per group), were mounted in the Instron ElectroPuls E10, 000 (Instron, Bucks, UK) using the same apparatus as the strain rate study. A 1 kN load cell was employed in this study due to a reduced load range. Specimens were loaded using a sinusoidal wave form between 1 and 5 MPa, while a frequency sweep was performed. This consisted of increasing the loading frequency by intervals of 0.2 Hz until 2 Hz was achieved, at which time testing ceased. The 5 MPa upper stress limit was deemed physiologically relevant due to the loads experienced by the ACL in-vivo (Fleming and Beynnon, 2004; Hosseini et al., 2011; Shelburne et al., 2004) and its cross-sectional area (Hashemi et al., 2005). This limit was used in a previous study investigating the viscoelastic properties of pSFT following different treatments (Herbert et al., 2015). 2 Hz was selected as an upper limit to normal walking speed in daily activities. Throughout testing, integrated DMA software continuously calculated and recorded the dynamic

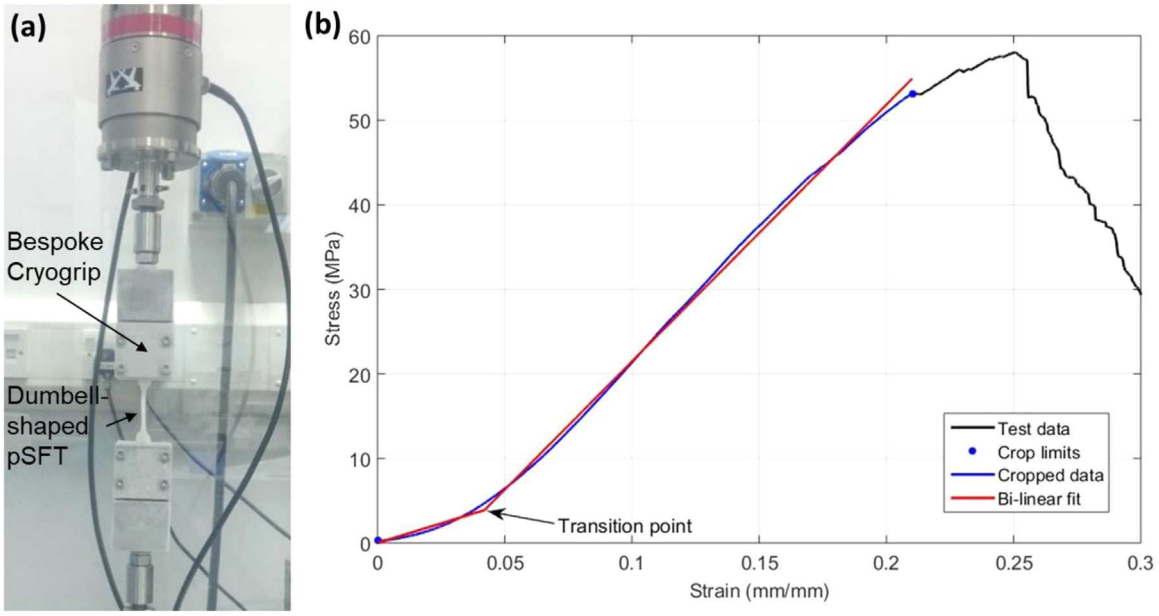

Fig. 1. (a) Testing set up used for varying strain rate and DMA tests. (b) Example of the bi-linear model applied to stress-strain data for the failure tests performed at varying strain rates (study 1).

modulus (E^*), storage modulus (E'), loss modulus (E'') and the damping ability (tan δ).

2.3. Statistical analyses

For both studies, statistical variances between groups were determined using a two-way analysis of variance (ANOVA). Tukey's significant difference test was used for post-hoc evaluation. A p-value of < 0.05 was considered to be statistically significant.

The data associated with this paper (including raw data, model input files and results) are openly available from the University of Leeds Data Repository (Edwards and Herbert, 2018).

3. Results

3.1. Study 1: strain rate dependency

The *UTS* and failure strain results of the strain rate dependency study are shown in Figs. 2a and 2b. *UTS* was significantly reduced in decellularised compared to native pSFT, whereas strain rate did not affect *UTS* in either test group. Failure strains were not significantly different regardless of test group or strain rate. No significant interactions were found between test groups and strain rate for either *UTS* or failure strain. The results for the toe region and linear region moduli (E_0 and E_1) are shown in Figs. 2c and 2d. E_0 was strain rate dependent in native tissue, but this was absent in decellularised pSFT. Decellularised pSFT had significantly lower toe region moduli than native tissue when tested at higher strain rates, and there was a significant interaction between strain rate and tissue type. E_1 was significantly lower in decellularised than native pSFT, but neither native nor decellularised tissues showed any significant strain rate dependency.

The results for the transition point coordinates are shown in Table 1. Transition stress (σ_T) appeared to be strain rate dependent in native tissues, although differences only reached significance between highest and lowest strain rates. Decellularised tissues only had significantly lower values for σ_T at the lowest strain rate. The transition strain (ε_T) was reduced significantly in native tissues at medium and high strain rates when compared to the lowest. A significant interaction between test group and strain rate was found for ε_T but not for σ_T.

3.2. Study 2: Dynamic Mechanical Analysis

The results of the dynamic mechanical analysis testing are shown in Figs. 3a to 3d. For the dynamic modulus (E^*), storage modulus (E') and loss modulus (E''), values for decellularised pSFT were significantly lower than native tissue. No signicant differences were found between the damping ability ($tan\,\delta$) of test groups (Fig. 3d). Only $E'''$and $tan\,\delta$ varied with frequency; compared to 0.2 Hz, significant decreases were seen in both native (E'', $tan\,\delta$) and decellularised tissues ($tan\,\delta$ only) at all other frequencies. No significant interactions were found between test groups and frequency.

4. Discussion

Decellularised xenogeneic tissues provide promising alternatives to standard autograft or allograft tissues in many applications, reducing the risk of necrosis and adverse immune responses due to the presence of dead donor cells. Following decellularisation, these tissues should be assessed to ensure that they are able to withstand the biomechanical conditions typical of their targeted in vivo environment (Desai et al., 2018). One of the most inherent characteristics of biological tissues is their viscoelasticity, which governs their strain rate dependent and dynamic biomechanical properties. However, the effects of decellularisation on these fundamental and vital functional parameters have yet to be investigated. Tendon has a complex hierarchical architecture, primarily comprising of type I collagen in addition to cells and non-collagenous molecules such as glycosaminoglycans (GAGs) (Screen et al., 2005). The decellularisation process has the potential to affect ECM structural elements in addition to removing cellular material, in turn affecting the viscoelastic properties. Changes in the viscoelastic properties of pSFT following decellularisation were seen in a previously reported study on bioburden reduction methods (Herbert et al., 2015).

When statistical analyses were made between native and decellularised groups, significant decreases due to decellularisation were seen for the elastic moduli (E_0, E_1) and tensile strength (*UTS*) of pSFT (Fig. 1a, c and d). This is not overly surprising as decellularisation protocols have previously been found to cause significant alterations to the ECM in a variety of biological tissues (Crapo et al., 2011; Gilbert et al., 2006), including loss of GAGS and the cleavage or crosslinking of collagen and elastin fibrils. Previous work by our group has shown

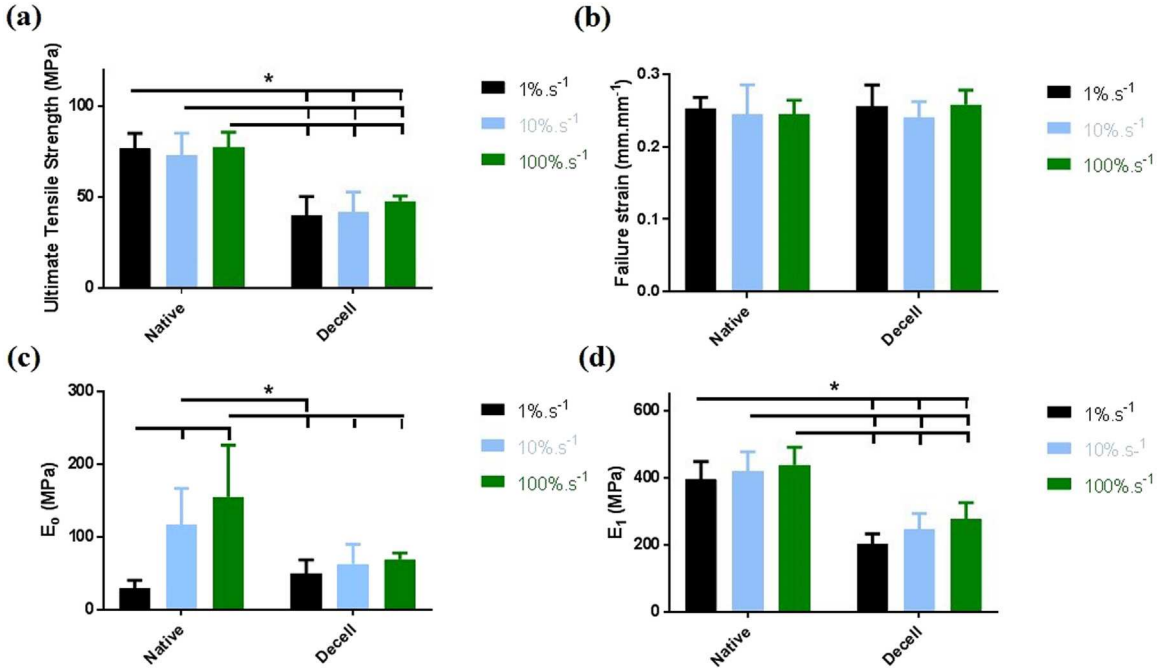

Fig. 2. Strain rate dependency results of study 1 (mean ± 95% CI, n = 6), (a) Ultimate tensile strength, (b) failure strain, (c) toe region modulus and (d) linear region modulus. Decell indicates decellularised group. * indicates significant difference ($P < 0.05$, 1-way ANOVA with Tukey post-hoc analysis).

similar reductions in biomechanical properties of the pSFT (Herbert et al., 2017, 2015) with decellularisation maintaining collagen content but causing a significant reduction in glycosaminoglycan (GAG) content (circa 75%; (Jones et al., 2017)).

The mechanical role of GAG sidechains in tendon is somewhat disputed, particularly as potential collagen fibril cross-linkers (Fessel and Snedeker, 2009; Rigozzi et al., 2013). Others theorise that GAGs can have a significant effect on tendon mechanical properties (Clemmer et al., 2010; Dunkman et al., 2013; Ryan et al., 2015; Screen et al., 2006, 2005). The present study found a reduction in the biomechanical properties of decellularised pSFT, which was produced using a method shown previously to reduce the GAG content (Jones et al., 2017). Swelling of decellularised pSFT was visually apparent but no quantitative measurements were recorded. The decellularisation process employed in this study involves dynamically washing for lengthy periods, providing abundant time for PBS to penetrate and swell the tissue despite the loss of GAGs. It is postulated that this mechanism of swelling increased the cross-sectional area of the decellularised pSFT but, as the ECM density within remained unchanged, the material properties were reduced.

In the absence of sufficient GAGs, collagen fibrils and their sub-fibrillar molecular crosslinks may be called upon to maintain structural integrity the ECM and has previously been suggested that decellularisation may affect these molecular crosslinks (Herbert et al., 2015). Collagen fibrils are stabilised by inter- and intra-molecular enzymatic crosslinks initially formed as unstable, immature divalent bonds which over time mature into stable, trivalent bonds (Couppe et al., 2009; Depalle et al., 2015; Patterson-Kane et al., 1997; Svensson et al., 2013). With a greater proportion of immature crosslinks likely to exist in the juvenile pSFT used in this study, the tissue may be susceptible to collagen matrix disruption caused by the decellularisation bioprocesses, including the peracetic acid wash step.

Another possible explanation for the reduction of the pSFT toe region and linear region moduli is that decellularisation may alter the extension behaviour of the collagen. Collagen crimping may be mediated by cell contraction between fibres (Herchenhan et al., 2012) and provides the initial non-linear load response under extension (Miller et al., 2012a, 2012b). Removal of the native cell population could therefore have implications for the maintenance of collagen crimp. Crimp straightening in combination with fibre extension is believed to be the principle mechanistic contributor to extension in the toe region of loading, while sliding of fibres is believed to be more pronounced in the linear region (Screen et al., 2004). We have previously proposed that pSFT collagen crimp periodicity is altered by decellularisation, increasing the toe region extensibility, explaining the reduction in the toe region modulus (E_0) (Herbert et al., 2015). With the reduction in the linear region modulus (E_1) seen in this study, decellularisation may also affect the fibre sliding mechanism prominent in linear region extensions. Continuous collagen fibres are not necessary for mechanical integrity and strength so long as the shear forces along and between the fibres are equal to the tensile forces along their length (Screen et al., 2006). Reduced fibre sliding acting within a swollen tissue may have diluted the protective shear effect between fibres, hence reducing the elastic moduli and tensile strength.

Increased strain rate was not found to affect the linear region modulus (E_1), ultimate tensile strength (UTS) or failure strain of native

Table 1
Transition point coordinate results of study 1 (mean ± 95% CI). Superscripts indicate significance – groups that do not share the same letter are significantly different ($P < 0.05$, 2-way ANOVA with Tukey post-hoc analysis).

	ε_T (mm.mm^{-1})			σ_T (MPa)		
Group	**1%.s^{-1}**	**10%.s^{-1}**	**100%.s^{-1}**	**1%.s^{-1}**	**10%.s^{-1}**	**100%.s^{-1}**
Native	0.029 ± 0.014^{a}	0.014 ± 0.005^{c}	0.016 ± 0.005^{b,c}	0.86 ± 0.39^{b}	1.46 ± 0.52^{a,b}	2.23 ± 0.76^{a}
Decell	0.028 ± 0.004^{a,b}	0.035 ± 0.010^{a}	0.027 ± 0.007^{a,b}	1.36 ± 0.60^{a,b}	2.21 ± 1.39^{a}	1.84 ± 0.55^{a,b}

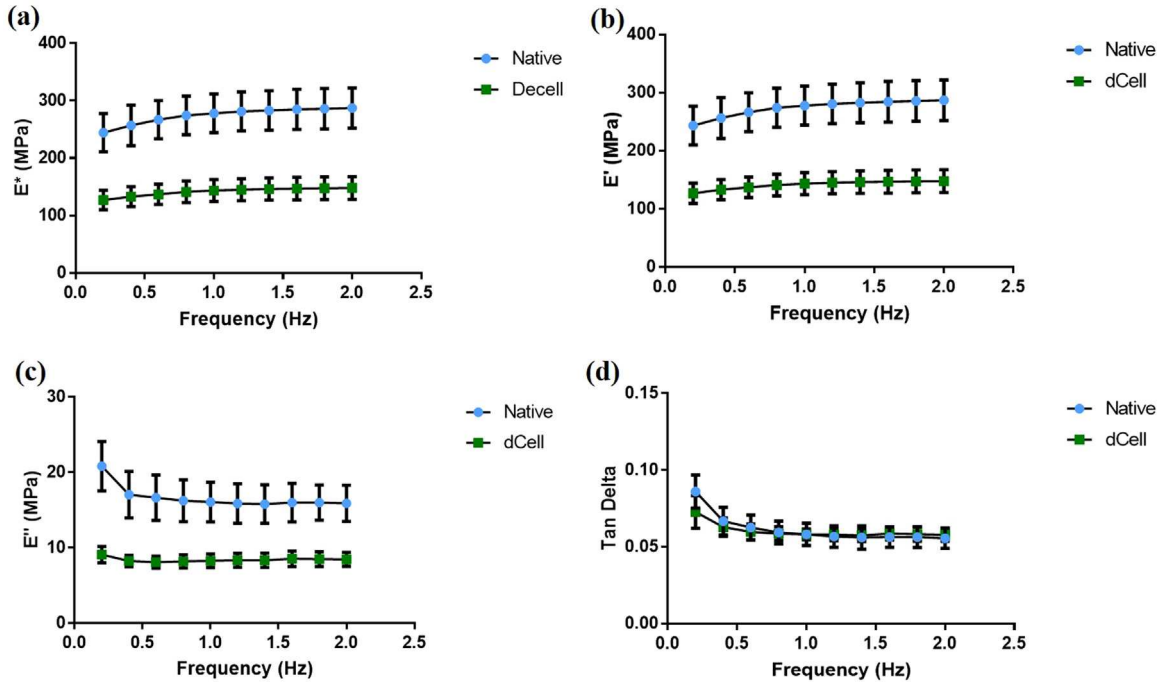

Fig. 3. Dynamic mechanical analysis results of study 2 (mean ± 95% CI, n = 6), (a) dynamic modulus, (b) storage modulus, (c) loss modulus and (d) damping ability. Decell indicates decellularised group. * indicates significant difference ($P < 0.05$, 1-way ANOVA with Tukey post-hoc analysis).

or decellularised pSFT. Although it may appear unusual that a strain rate dependent effect was not discovered for the linear region modulus of decellularised or native pSFT, this has also been observed in human patellar tendon (Blevins et al., 1994) and ovine flexor tendon (Lynch et al., 2003). Other studies have shown that increasing strain rate can increase the linear modulus in cervical spine ligaments (Mattucci et al., 2012), increase failure force and stiffness in craniovertebral ligaments (Mattucci et al., 2013), increase linear modulus and tensile strength in lateral collateral knee ligaments (Bonner et al., 2015) and increase both toe region and linear region moduli in anterior rectus (Ben Abdelounis et al., 2013). Together, these studies suggest that the strain rate dependency of individual mechanical properties may be highly tissue specific.

The testing in this study was completed at a whole tendon level, which includes the endotendon that surrounds collective fascicles and may contribute to the strain rate dependent and dynamic mechanical properties of the tissue. One possible explanation for the decline in the strain dependent response in toe region modulus (E_0) seen in this study is that the removal of cells and ECM changes (such as GAG loss) result in a more open porous medium, reducing viscous drag as fluid can flow through the tissue more readily, even at faster rates of loading. This would also explain the significant interaction between test group and strain rate for transition strain (ε_T) (Table 1).

Dynamic mechanical analysis allows for the separation of a tissue's dynamic modulus (E^*) at different frequencies into its viscous fluid (loss modulus) and solid elastic (storage modulus) phase components (E'' & E' respectively), giving an insight into how much fluid and ECM content contribute at different loading rates. Additionally, the damping ability ($\tan\delta$; the ratio of E'' to E') provides a measure of energy loss and force transfer efficiency. Significant reductions were found for dynamic, storage and loss moduli at all frequencies measured (Fig. 2a–c). The loss modulus (E'') was also found to interact with frequency, reducing to steady state conditions with increasing frequency. This reduction appeared more pronounced in the native tissue group indicating a larger initial fluid phase contribution at low deformation rates compared to decellularised tissues. This complements the toe region modulus strain rate dependency results in study 1 and the theory that decellularisation causes an increase in internal fluid flow and dissipation. Previous studies have concluded that the dynamic mechanical responses of tendon are not GAG mediated (Fessel and Snedeker, 2009), but more likely to be mediated by collagen uncrimping (Buckley et al., 2013) or cross-linking (Nagasawa et al., 2008), areas which we theorise may have been affected by decellularisation. Interestingly, no significant difference was found for the damping ability ($\tan\delta$) between native and decellularised groups, indicating that the force transfer efficiency remained unchanged. As this parameter is calculated by the ratio of E'' to E', it appears that changes in the loss and storage moduli of the pSFT were proportionally similar following decellularisation. This may provide evidence that the effects of decellularisation on the solid and fluid phase components of the tissue are interlinked and that by affecting one, the other is intrinsically affected.

Limitations with the studies presented arise as testing for both study 1 and study 2 were performed utilising the same mechanical testing system, with strain was measured using crosshead displacement rather than video extensometry. However, previous work has found extreme difficulty in labelling this tissue with sufficient contrast to effectively trace markers with an infrared camera. Furthermore, the specimen dumbbell configuration presumes that preferential deformation occurs at the thinned gauge length section and that this equates to the crosshead displacement. Future work investigating the effects of extended PBS washes on pSFT, as well as more detailed microscopic analysis of the collagen structure following decellularisation, would help to identify structural changes within the tissue which may be responsible for changes in their biomechanical properties.

In conclusion, decellularisation has been found to affect the strain rate dependent and dynamic mechanical properties of pSFT. Despite these changes, ample strength and integrity remains for the tissue to act as a viable regenerative ACL replacement graft. At the time of writing, this is to the authors' knowledge the first study to utilise strain rate dependency testing and dynamic mechanical analysis in a combined approach to assess the effects of decellularisation on biological tissue. This study contributes to understanding of how the decellularisation process may affect ligamentous tissues and provides further data on their complex material properties. This data is vital for encouraging

clinical translation of these grafts and will also be used for development of computational models of their behaviour following ACL reconstruction.

Acknowledgements

Funding: This work was supported with an Engineering and Physical Sciences Research Council (EPSRC, UK) ETERM Landscape Fellowship (EP/I017801/1) and an EPSRC Programme Grant (Optimising Knee Therapies; EP/P001076/1). Part of this research was also supported by the National Institute for Health Research (NIHR, UK) Leeds Musculoskeletal Biomedical Research Unit. The views expressed are those of the author(s) and not necessarily those of the NHS, the NIHR or the Department of Health.

References

Ben Abdelounis, H., Nicolle, S., Ottenio, M., Beillas, P., Mitton, D., 2013. Effect of two loading rates on the elasticity of the human anterior rectus sheath. J. Mech. Behav. Biomed. Mater. 20, 1–5.

Blevins, F.T., Hecker, A.T., Bigler, G.T., Boland, A.L., Hayes, W.C., 1994. The effects of donor age and strain-rate on the biomechanical properties of bone-patellar tendon-bone allografts. Am. J. Sport Med. 22, 328–333.

Bonner, T.J., Newell, N., Karunaratne, A., Pullen, A.D., Amis, A.A., 2015. Strain-rate sensitivity of the lateral collateral ligament of the knee. J. Mech. Behav. Biomed. Mater. 41, 261–270.

Booth, C., Korossis, S.A., Wilcox, H.E., Watterson, K.G., Kearney, J.N., Fisher, J., Ingham, E., 2002. Tissue engineering of cardiac valve prostheses I: development and histological characterization of an acellular porcine scaffold. J. Heart Valve Dis. 11, 457–462.

Buckley, M.R., Sarver, J.J., Freedman, B.R., Soslowsky, L.J., 2013. The dynamics of collagen uncrimping and lateral contraction in tendon and the effect of ionic concentration. J. Biomech. 46, 2242–2249.

Chandrashekar, N., Hashemi, J., Slauterbeck, J., Beynnon, B.D., 2008. Low-load behaviour of the patellar tendon graft and its relevance to the biomechanics of the reconstructed knee. Clin. Biomech. 23, 918–925.

Clemmer, J., Liao, J., Davis, D., Horstemeyer, M.F., Williams, L.N., 2010. A mechanistic study for strain rate sensitivity of rabbit patellar tendon. J. Biomech. 43, 2785–2791.

Couppe, C., Hansen, P., Kongsgaard, M., Kovanen, V., Suetta, C., Aagaard, P., Kjaer, M., Magnusson, S.P., 2009. Mechanical properties and collagen cross-linking of the patellar tendon in old and young men. J. Appl. Physiol. 107, 880–886.

Crapo, P.M., Gilbert, T.W., Badylak, S.F., 2011. An overview of tissue and whole organ decellularization processes. Biomaterials 32, 3233–3243.

Depalle, B., Qin, Z., Shefelbine, S.J., Buehler, M.J., 2015. Influence of cross-link structure, density and mechanical properties in the mesoscale deformation mechanisms of collagen fibrils. J. Mech. Behav. Biomed. Mater. 52, 1–13.

Desai, A., Vafaee, T., Rooney, P., Kearney, J.N., Berry, H.E., Ingham, E., Fisher, J., Jennings, L.M., 2018. In vitro biomechanical and hydrodynamic characterisation of decellularised human pulmonary and aortic roots. J. Mech. Behav. Biomed. Mater. 79, 53–63.

Dunkman, A.A., Buckley, M.R., Mienaltowski, M.J., Adams, S.M., Thomas, S.J., Satchell, L., Kumar, A., Pathmanathan, L., Beason, D.P., Iozzo, R.V., Birk, D.E., Soslowsky, L.J., 2013. Decorin expression is important for age-related changes in tendon structure and mechanical properties. Matrix Biol. 32, 3–13.

Edwards, J.H., Herbert, A., 2018. Strain Rate Dependant and Dynamic Mechanical Properties of Porcine Superflexor Tendons [dataset]. University of Leeds Data Repository, UK. https://doi.org/10.5518/467.

Edwards, J.H., Herbert, A., Jones, G.L., Manfield, I.W., Fisher, J., Ingham, E., 2016. The effects of irradiation on the biological and biomechanical properties of an acellular porcine superflexor tendon graft for cruciate ligament repair. J. Biomed. Mater. Res. Part B, Appl. Biomater. https://doi.org/10.1002/jbm.b.33786.

Fessel, G., Snedeker, J.G., 2009. Evidence against proteoglycan mediated collagen fibril load transmission and dynamic viscoelasticity in tendon. Matrix Biol. 28, 503–510.

Fleming, B.C., Beynnon, B.D., 2004. In vivo measurement of ligament/tendon strains and forces: a review. Ann. Biomed. Eng. 32, 318–328.

Fradet, L., Cliche, F., Petit, Y., Mac-Thiong, J.M., Arnoux, P.J., 2016. Strain rate dependent behavior of the porcine spinal cord under transverse dynamic compression. Proc. Inst. Mech. Eng. Part H.-J. Eng. Med. 230, 858–866.

Gaur, P., Chawla, A., Verma, K., Mukherjee, S., Lalvani, S., Malhotra, R., Mayer, C., 2016. Characterisation of human diaphragm at high strain rate loading. J. Mech. Behav. Biomed. Mater. 60, 603–616.

Gilbert, T.W., Sellaro, T.L., Badylak, S.F., 2006. Decellularization of tissues and organs. Biomaterials 27, 3675–3683.

Hashemi, J., Chandrashekar, N., Cowden, C., Slauterbeck, J., 2005. An alternative method of anthropometry of anterior cruciate ligament through 3-D digital image reconstruction. J. Biomech. 38, 551–555.

Hatami-Marbini, H., Rahimi, A., 2015. Collagen cross-linking treatment effects on corneal dynamic biomechanical properties. Exp. Eye Res. 135, 88–92.

Herbert, A., Brown, C., Rooney, P., Kearney, J., Ingham, E., Fisher, J., 2016. Bi-linear mechanical property determination of acellular human patellar tendon grafts for use in anterior cruciate ligament replacement. J. Biomech. 49, 1607–1612.

Herbert, A., Edwards, J.H., Jones, G.L., Ingham, E., Fisher, J., 2017. The effects of irradiation dose and storage time following treatment on the viscoelastic properties of decellularised porcine super flexor tendon. J. Biomech. 57, 157–160.

Herbert, A., Jones, G.L., Ingham, E., Fisher, J., 2015. A biomechanical characterisation of acellular porcine super flexor tendons for use in anterior cruciate ligament replacement: investigation into the effects of fat reduction and bioburden reduction bio-processes. J. Biomech. 48, 22–29.

Herchenhan, A., Kalson, N.S., Holmes, D.F., Hill, P., Kadler, K.E., Margetts, L., 2012. Tenocyte contraction induces crimp formation in tendon-like tissue. Biomech. Model. Mechanobiol. 11, 449–459.

Hosseini, A., Gill, T.J., Van de Velde, S.K., Li, G., 2011. Estimation of in vivo ACL force changes in response to Increased weightbearing. J. Biomech. Eng.-Trans. Asme 133.

Jin, X., Zhu, F., Mao, H.J., Shen, M., Yang, K.H., 2013. A comprehensive experimental study on material properties of human brain tissue. J. Biomech. 46, 2795–2801.

Jones, G.L., Herbert, A., Berry, H., Edwards, J.H., Fisher, J., Ingham, E., 2017. Decellularisation and characterisation of porcine superflexor tendon: a potential anterior cruciate ligament replacement. Tissue Eng. Part A 23, 124–134.

Joyce, C.D., Randall, K.L., Mariscalco, M.W., Magnussen, R.A., Flanigan, D.C., 2015. Bone-patellar tendon-bone versus soft-tissue allograft for anterior cruciate ligament reconstruction: a systematic review. Arthroscopy.

Kiapour, A.M., Murray, M.M., 2014. Basic science of anterior cruciate ligament injury and repair. Bone Jt. Res. 3, 20–31.

Knight, R.L., Booth, C., Wilcox, H.E., Fisher, J., Ingham, E., 2005. Tissue engineering of cardiac valves: Re-seeding of acellular porcine aortic valve matrices with human mesenchymal progenitor cells. J. Heart Valve Dis. 14, 806–813.

Lynch, H.A., Johannessen, W., Wu, J.P., Jawa, A., Elliott, D.M., 2003. Effect of fiber orientation and strain rate on the nonlinear uniaxial tensile material properties of tendon. J. Biomech. Eng.-Trans. Asme 125, 726–731.

Macaulay, A.A., Perfetti, D.C., Levine, W.N., 2012. Anterior cruciate ligament graft choices. Sports Health 4, 63–68.

MacManus, D.B., Pierrat, B., Murphy, J.G., Gilchrist, M.D., 2015. Dynamic mechanical properties of murine brain tissue using micro-indentation. J. Biomech. 48, 3213–3218.

Mattucci, S.F.E., Moulton, J.A., Chandrashekar, N., Cronin, D.S., 2012. Strain rate dependent properties of younger human cervical spine ligaments. J. Mech. Behav. Biomed. Mater. 10, 216–226.

Mattucci, S.F.E., Moulton, J.A., Chandrashekar, N., Cronin, D.S., 2013. Strain rate dependent properties of human craniovertebral ligaments. J. Mech. Behav. Biomed. Mater. 23, 71–79.

Miller, K.S., Connizzo, B.K., Feeney, E., Soslowsky, L.J., 2012a. Characterizing local collagen fiber re-alignment and crimp behavior throughout mechanical testing in a mature mouse supraspinatus tendon model. J. Biomech. 45, 2061–2065.

Miller, K.S., Connizzo, B.K., Feeney, E., Tucker, J.J., Soslowsky, L.J., 2012b. Examining differences in local collagen fiber crimp frequency throughout mechanical testing in a developmental mouse supraspinatus tendon model. J. Biomech. Eng.-Trans. Asme 134.

Nagasawa, K., Noguchi, M., Ikoma, K., Kubo, T., 2008. Static and dynamic biomechanical properties of the regenerating rabbit Achilles tendon. Clin. Biomech. 23, 832–838.

Ottenio, M., Tran, D., Annaidh, A.N., Gilchrist, M.D., Bruyere, K., 2015. Strain rate and anisotropy effects on the tensile failure characteristics of human skin. J. Mech. Behav. Biomed. Mater. 41, 241–250.

Patterson-Kane, J.C., Parry, D.A.D., Birch, H.L., Goodship, A.E., Firth, E.C., 1997. An age-related study of morphology and cross-link composition of collagen fibrils in the digital flexor tendons of young thoroughbred horses. Connect. Tissue Res. 36, 253–260.

Pinkowski, J.L., Rodrigo, J.J., Sharkey, N.A., Vasseur, P.B., 1996. Immune response to nonspecific and altered tissue antigens in soft tissue allografts. Clin. Orthop. Relat. Res. 326, 80–85.

Rigozzi, S., Muller, R., Stemmer, A., Snedeker, J.G., 2013. Tendon glycosaminoglycan proteoglycan sidechains promote collagen fibril sliding-AFM observations at the nanoscale. J. Biomech. 46, 813–818.

Ryan, C.N.M., Sorushanova, A., Lomas, A.J., Mullen, A.M., Pandit, A., Zeugolis, D.I., 2015. Glycosaminoglycans in tendon physiology, pathophysiology, and therapy. Bioconjugate Chem. 26, 1237–1251.

Screen, H.R.C., Chhaya, V.H., Greenwald, S.E., Bader, D.L., Lee, D.A., Shelton, J.C., 2006. The influence of swelling and matrix degradation on the microstructural integrity of tendon. Acta Biomater. 2, 505–513.

Screen, H.R.C., Lee, D.A., Bader, D.L., Shelton, J.C., 2004. An investigation into the effects of the hierarchical structure of tendon fascicles on micromechanical properties. Proc. Inst. Mech. Eng. Part H.-J. Eng. Med. 218, 109–119.

Screen, H.R.C., Shelton, J.C., Chhaya, V.H., Kayser, M.V., Bader, D.L., Lee, D.A., 2005. The influence of noncollagenous matrix components on the micromechanical environment of tendon fascicles. Ann. Biomed. Eng. 33, 1090–1099.

Shelburne, K.B., Pandy, M.G., Anderson, F.C., Torry, M.R., 2004. Pattern of anterior cruciate ligament force in normal walking. J. Biomech. 37, 797–805.

Stapleton, T.W., Ingram, J., Katta, J., Knight, R., Korossis, S., Fisher, J., Ingham, E., 2008. Development and characterization of an acellular porcine medial meniscus for use in tissue engineering. Tissue Eng. Part A 14, 505–518.

Svensson, R.B., Mulder, H., Kovanen, V., Magnusson, S.P., 2013. Fracture mechanics of collagen fibrils: influence of natural cross-links. Biophys. J. 104, 2476–2484.

Woo, S.L.Y., Danto, M.I., Ohland, K.J., Lee, T.Q., Newton, P.O., 1990. The use of a laser micrometer system to determine the cross-sectional shape and area of ligaments - a comparative study with 2 existing methods. J. Biomech. Eng.-Trans. Asme 112, 426–431.